Hierarchical self-assembly of nematic colloidal superstructures

M. Škarabot,[1] M. Ravnik,[2] S. Žumer,[1,2] U. Tkalec,[1] I. Poberaj,[2] D. Babič,[2] and I. Muševič[1,2,*]
[1]*J. Stefan Institute, Jamova 39, 1000 Ljubljana, Slovenia*
[2]*Faculty of Mathematics and Physics, University of Ljubljana, Jadranska 19, 1000 Ljubljana, Slovenia*
(Received 10 October 2007; published 12 June 2008)

We show that colloidal superstructures could be assembled in mixtures of large and small colloidal particles dispersed in a nematic liquid crystal. Using elastic interaction of small colloidal particles with the disclination lines we succeed to demonstrate how one can decorate with small particles a topological matrix of defect rings and loops formed by an array of large colloidal particles. Our simulations show that this concept of colloidal self-assembly in nematics could be extended down to the nanoscale particles.

DOI: 10.1103/PhysRevE.77.061706 PACS number(s): 61.30.Jf, 47.57.J−

Nematic liquid crystals (NLC) are orientationally ordered complex fluids [1], in which rodlike molecules are spontaneously aligned into a certain direction, called the director. An inclusion, such as a spherical colloidal particle, creates a disturbance in the local orientation of the NLC, because of its interaction with the surface of the inclusion [2–4]. Due to the topological conservation laws [5,6], such a disturbance is spatially strongly anisotropic even though the colloidal particles are spherical, and spreads over micrometer distances. When several colloidal particles are brought together in the NLC, the total energy of the system depends on particle separation, which means that a force of structural origin emerges between the particles [4,7]. These forces have been used for "decorating" liquid crystalline surfaces [1,8] but it has recently been shown that they give rise to some fascinating one-dimensional and two-dimensional self-assembled colloidal structures [9,10], with a typical binding energy of several $1000k_BT$ per micrometer-sized particle. The extremely strong and anisotropic binding of the nematic colloids by the structural forces makes these systems technologically very promising for future applications of colloids in photonic devices [11]. However, it has remained unexplored whether the topological properties of liquid crystals could be used to self-assemble particles of very different sizes and material properties into colloidal superstructures.

Topological defects in the NLC are characterized by the reduced nematic and increased biaxial order in the core of the defects, as well as the highly distorted nematic director in the vicinity of the defect lines [1]. It is well known that topological defect in the form of a Saturn ring can form spontaneously around a spherical particle [12]. Now, if we consider a smaller colloidal particle and approach it to the original Saturn ring, it is expected to be more favorable for the smaller particle to migrate into the core of the Saturn ring defect [13,14] as it will reduce the volume with director distortion and consequently, also the total free energy. Here we show that various colloidal superstructures could indeed be hierarchically self-assembled in nematic colloids of different sizes using nematic elasticity. We demonstrate two types of colloidal superstructures: a Saturn ring filled with smaller colloidal particles, and a decorated entangled colloidal loop [15–18], encircling two or several colloidal particles.

The experiments have been performed by confining nematic colloids into thin planar or homeotropic glass cells of thicknesses from 5 to 22 μm, which were providing strong either parallel or perpendicular orientation of the NLC pentylcyanobiphenyl (5CB) at the cell walls. The surfaces of larger colloidal particles (glass microspheres of diameter 19 μm and silica spheres of diameter 10 μm) were covered with a monolayer of silane DMOAP (N,N-dimethyl-N-octadecyl-3-aminopropyl-trimetoxysilyl chloride) to induce local perpendicular alignment of liquid crystal molecules [10]. When the cell thickness was comparable to the diameter of larger colloidal particles, the NLC adopted the "Saturn ring" configuration [10,12], with a topological defect in the form of a defect ring with the winding number $-1/2$ and topological charge of magnitude 1, encircling the particle at its equator.

To prove the concept of hierarchical ordering, first the interaction between two different-sized particles was studied. Using the laser tweezers a smaller silica colloidal particle of 1.5 μm diameter with a homeotropically treated surface, was positioned close to the Saturn ring of a larger colloidal particle and released. Figure 1(a) presents a sequence of microscope images, which clearly reveal that the smaller colloidal particle is strongly attracted into the Saturn ring of the larger particle. In this series of images, colloidal particles of 19 μm diameter were embedded in a 22 μm-thick planar nematic cell. From the recorded sequence of images in Fig. 1(a), we have calculated [19] the attractive potential between the smaller colloidal particle and the Saturn ring, which is presented in Fig. 1(b).

The interaction between smaller and larger colloids was studied using Landau-de Gennes (LdG) expansion [1,18] of the free energy F as follows:

$$F = +\frac{1}{2}K\int_{LC}\left(\frac{\partial Q_{ij}}{\partial x_k}\right)\left(\frac{\partial Q_{ij}}{\partial x_k}\right)dV + \int_{LC}\left(\frac{1}{2}AQ_{ij}Q_{ji} + \frac{1}{3}BQ_{ij}Q_{jk}Q_{ki} + \frac{1}{4}C(Q_{ij}Q_{ji})^2\right)dV + \frac{1}{2}W\int_{surf.\ col.}(Q_{ij}-Q_{ij}^0)(Q_{ji}-Q_{ji}^0)dS. \quad (1)$$

*igor.musevic@ijs.si

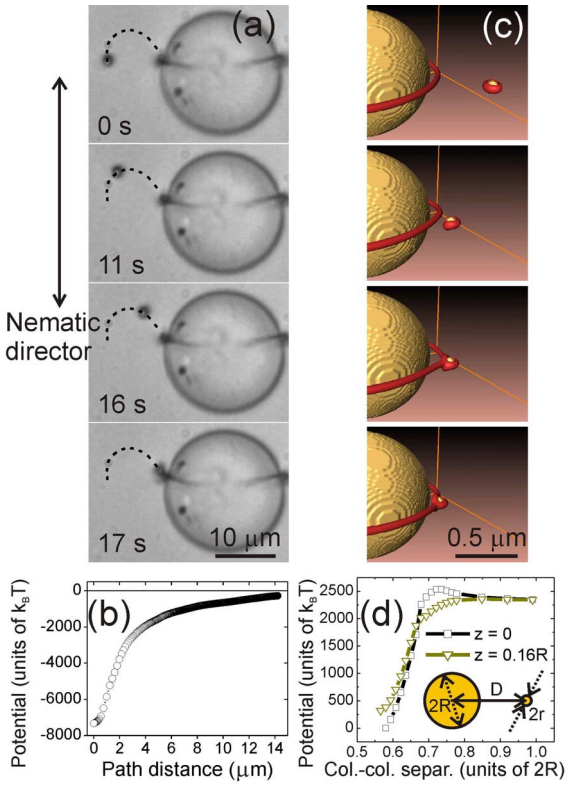

FIG. 1. (Color online) (a) Small colloidal particle of 1.5 μm diameter is attracted into the Saturn ring of a 19 μm colloidal particle, following the black dashed path. (b) Binding potential of the small colloidal particle along the trapping path. (c) Numerical calculation: a 100 nm nanoparticle is attracted into the Saturn ring around a 1 μm colloidal particle. (d) The calculated binding potential of the small particle as a function of the particle-particle separation for trajectories at different off-centeredness "z" from the central xy plane. Note the qualitative matching between the theory and experiments.

The first term describes the increase of the free energy due to spatial variations of the nematic orientation and order; the second term represents the contribution to F due to the magnitude of the nematic order; and the third term couples the nematic with surfaces. We have chosen a single elastic constant approximation (K); A, B, and C are the material constants, W is the strength of the surface anchoring, and Q_{ij}^0 is the order parameter preferred by the surface. The equilibrium tensorial order parameter field was found by solving the corresponding set of Euler-Lagrange equations using an explicit relaxation algorithm on a cubic mesh with 10 nm resolution [20]. During the tensor relaxation procedure, positions of all colloidal particles were fixed and their surfaces imposed preferred homeotropic orientation. When relaxed, the free energy of the system was calculated from the equilibrium order parameter field. The procedure was repeated by slightly changing the positions of the particles, which finally resulted in a free-energy landscape with potential minima representing stable states of the system. The following parameter values were used: $A=-0.172\times10^6$ J/m^3, $B=-2.12\times10^6$ J/m^3, $C=1.73\times10^6$ J/m^3 [21], and $W=1\times10^{-2}$ J/m^2 for all particle surfaces. The cell imposed strong homogeneous anchoring and was 2 μm thick. The larger colloidal particle diameter was $2R=1$ μm, and $K=4\times10^{-11}$ N.

A general configuration of colloidal particles, however, has typically low symmetry as well as a large number of degrees of freedom in particle positions, which have to be relaxed in order to find the equilibrium colloidal configuration. Therefore, we extended, for the more complex colloidal superstructures, the basic relaxation algorithm to include also particle "quasidynamics." Here the particles are free to move during the relaxation, however, in the calculation no material flow is included. Within the quasidynamical relaxation first the initial particle positions are chosen and then for a certain number of iteration steps in the order parameter relaxation (typically ~3000), which corresponds to the time interval Δt, the particles are fixed. After time Δt, the total elastic force $\mathcal{F}_i^{(j)}$ on the jth particle is calculated by integrating the Ericksen stress tensor σ_{ij} over the particle's surface $\mathcal{F}_i^{(j)}=\int_{surf}\sigma_{ji}dS_j$, where

$$\sigma_{ij}=-\frac{\partial f}{\partial\left(\frac{\partial Q_{kl}}{\partial x_i}\right)}\frac{\partial Q_{kl}}{\partial x_j}+\delta_{ij}f, \tag{2}$$

and f is total free energy volume density. We further assume overdamped particle dynamics, $\mathcal{F}_i^{(j)}=6\pi\eta R\Delta r_i^{(j)}/\Delta t$, where $\Delta r_i^{(j)}$ is now the jth particle shift in the ith direction. Note that by assuming the above friction force, inertia and possible sideways moves of the particles due to anisotropic viscosity are neglected. Having the particle shifts $\Delta r_i^{(j)}$ in the time interval Δt [22], we are now able to reposition all particles. After the repositioning, the algorithm loops iteratively, starting again with the order parameter relaxation with fixed, newly positioned particles.

Figure 1(c) presents several steps during the "numerical trapping" of a small colloidal particle into the Saturn ring of a larger colloidal particle. The corresponding interaction potential is shown in Fig. 1(d), and nicely reveals its anisotropy: if the small particle approaches the defect ring directly (see the $z=0$ curve), it has to overcome an energy barrier of several $100k_BT$; however, if it approaches slightly off the center (see the $z=0.16R$ curve), the energy barrier disappears. This explains why the trajectory of the small particle in Fig. 1(a) is curved, as it is attracted into the ring. Similar curved trajectories were observed by Pires *et al.* [13], and were explained by the symmetry properties of $-1/2$ defect lines.

The question arises, whether one could create a more sophisticated scaffold, or even network of decorated defect lines, connecting or surrounding several large colloidal particles. For this reason, we have used a high power laser beam of the laser tweezers [18] to heat the liquid crystal locally into the isotropic phase, and quenched it into the nematic phase by switching off the light. It has been shown in [18], that several types of entangled defects, surrounding and connecting two or more particles, can be formed in this way. We have chosen the "figure eight" entangled pair, shown in Fig. 2(a) as the most robust representative. Here, a perpendicular alignment of the NLC in the measuring cell was chosen, so that the Saturn rings now appear as dark circles in the plane

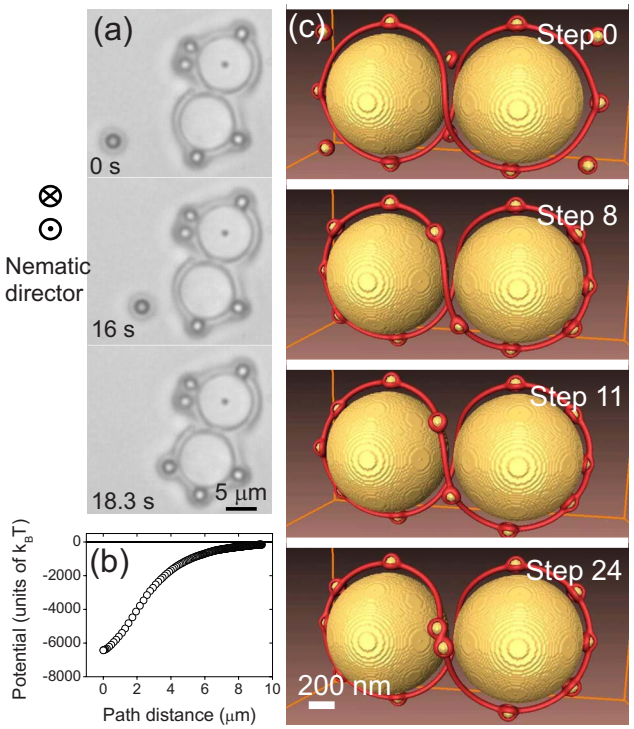

FIG. 2. (Color online) (a) Smaller colloidal particles of 2.32 μm are also strongly attracted into the figure eight defect loop. (b) The potential of smaller colloidal particles in the vicinity of the figure eight. (c) Trapping sequence of smaller 100 nm particles into the figure eight defect formed around a pair of 1 μm particles. Step 0 corresponds to the initial configuration and step 24 to the final configuration in the quasidynamical relaxation.

of the image, whereas an entangled $-1/2$ defect loop is a thin dark line encircling both colloidal particles in Fig. 2(a). One can notice from the sequence of images in Fig. 2(a), that a smaller colloidal particle (visible in the lower-left corner), which was positioned close to the entangled pair, is attracted into the defect loop. The corresponding potential is shown in Fig. 2(b) and is similar to the Saturn ring attraction in Fig. 1(a). Figure 2(c) shows the numerically modeled formation of a superstructure in the form of the "figure eight colloidal ring," where 100 nm colloidal particles are trapped into the "figure eight" entangled defect structure.

Spatial organization of smaller colloidal particles, assembled in the defect ring of the figure eight is shown in more detail in Fig. 3(a). The images were taken by slightly changing the depth of the focus, which clearly reveals that smaller particles are indeed trapped into the topological defect ring at different cell depths. The deformation of the director field around a similar superstructure, formed by smaller and larger colloidal particles, is clearly illustrated by the interference colors in Fig. 3(b) using a λ wave plate for the red light.

The observed colloidal superstructures are extremely interesting for application in metamaterials [23]. Figures 4(a) and 4(b) show the Saturn ring filled with small colloidal particles. Providing that the small particles are made of conductive material, such a structure could function as a distributed split ring resonator (SRR), with the electrical scheme

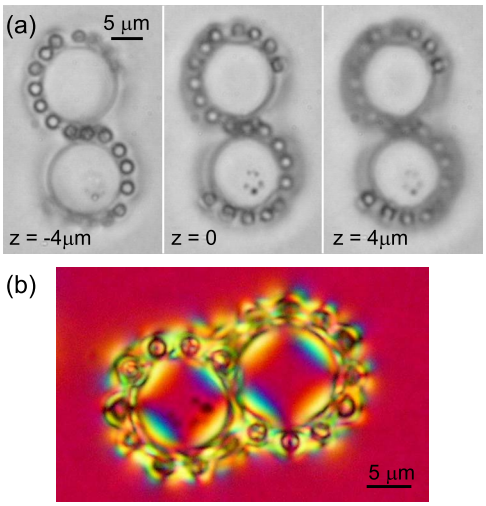

FIG. 3. (Color online) (a) Smaller colloidal particles are trapped into the topological defect loop, twisting around a larger colloidal pair (diameter 10 μm). Images were taken at different heights of the microscope focus. (b) Microscope image of birefringence, showing nematic distortion around the colloidal superstructure.

shown in the inset of Fig. 4(b). Here, the capacitor C is formed of the two conductive surfaces of the neighboring colloidal spheres in close proximity, filled with the NLC, whereas the inductance L comes from the small conductive colloidal particles. A series of conductive particles trapped

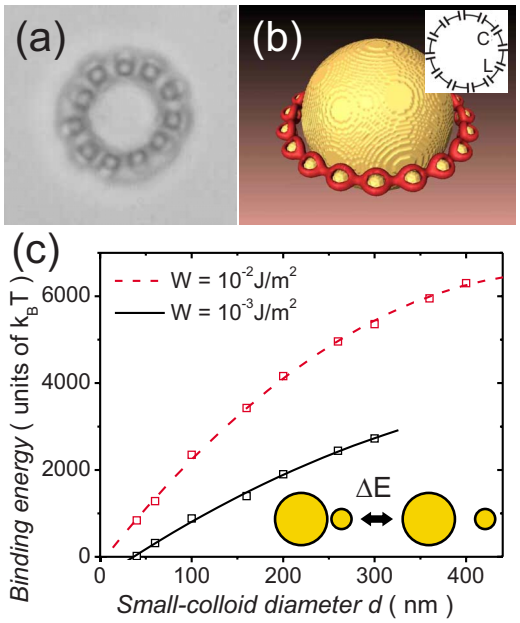

FIG. 4. (Color online) (a) Possible split ring resonator superstructure, formed of small colloidal particles trapped into the Saturn ring of the large particle. (b) A calculated stable colloidal ring superstructure of small 100 nm and a large 1 μm particle. The inset shows a schematic electrical circuit corresponding to a Saturn ring filled with conductive colloidal particles. (c) Calculated binding energy of a small particle with diameter d into the core of the Saturn ring, formed around a 1 μm colloidal particle for two different anchoring strengths W at the particle surfaces. Lines are parabolic fits.

into the ring, therefore represents a distributed *LC* circuit. An estimate shows that for a 5 μm diameter of the colloidal ring and 50 nm diameter small particles, the resonant frequency of the distributed resonant circuit is at the order of 15 THz, corresponding to the wavelength of 12 μm.

Scaling down to nanodimensions of the observed hierarchical ordering was explored using our LdG modeling. In Fig. 4(c) we show the binding energy of a single small particle into a Saturn ring depending on the small particle diameter d, as a measure down to which scales hierarchical ordering could be effective. Our estimate is that for very strong surface anchoring, self-assembly using structural forces could be effective down to a few nm colloidal particles.

The main result of our work is that various colloidal superstructures could be hierarchically self-assembled from the NLC with colloidal particles of different sizes. The basic mechanism of hierarchical self-assembly in the nematic colloids is simple: each foreign particle creates an orientational deformation in the NLC and is attracted to the scaffold of topological defects, which are inherently sources of strong nematic deformations. We have demonstrated two types of colloidal superstructures where small colloidal particles decorate a single Saturn-like ring, and an entangled loop encircling pair of large colloidal particles. Unlike forces that are responsible for the organization of colloidal particles in the isotropic solvents, the structural forces in the NLC colloids are anisotropic and can act on hierarchically chosen length scales originating from the intrinsic particle scales and anchoring strengths. This allows us to assemble predetermined colloidal superstructures using a scaffold of topological defect lines in the mixtures of large and small particles, with hierarchically chosen interactions ranging from micrometer to nanometer scale. The possible extension to different colloidal materials is obvious, as the colloidal interactions depend only on the surface properties of colloidal particles. A very fine balance between the local disorder and the elastic distortion controls the self-assembly. Although we have shown simple examples of colloidal superstructures, it is clear that complex and material-independent colloidal superstructures could be built.

[1] P. G. de Gennes and J. Prost, *The Physics of Liquid Crystals*, 2nd ed. (Oxford Science Publications, Oxford, 1993).

[2] R. B. Meyer, Mol. Cryst. Liq. Cryst. **16**, 355 (1972).

[3] E. M. Terentjev, Phys. Rev. E **51**, 1330 (1995).

[4] S. Ramaswamy, R. Nityananda, V. A. Raghunathan, and J. Prost, Mol. Cryst. Liq. Cryst. Sci. Technol., Sect. A **288**, 175 (1996).

[5] M. Kleman and O. D. Lavrentovich, Philos. Mag. **86**, 4117 (2006).

[6] H. Stark, Phys. Rep. **351**, 387 (2001).

[7] R. W. Ruhwandl and E. M. Terentjev, Phys. Rev. E **55**, 2958 (1997).

[8] P. E. Cladis and P. Pieranski, C. R. Seances Acad. Sci., Ser. B **273**, 275 (1971).

[9] P. Poulin, H. Stark, T. C. Lubensky, and D. A. Weitz, Science **275**, 1770 (1997).

[10] I. Muševič, M. Škarabot, U. Tkalec, M. Ravnik, and S. Žumer, Science **313**, 954 (2006).

[11] J. D. Joannopoulos, P. R. Villeneuve, and S. Fan, Nature (London) **386**, 143 (1997); V. W. A. de Villeneuve *et al.*, Science **309**, 1231 (2005); A. van Blaaderen, R. Ruel, and P. Wiltzius, Nature (London) **385**, 321 (1997); Y. A. Vlasov *et al.*, *ibid.* **414**, 289 (2001); M. E. Leunissen *et al.*, *ibid.* **437**, 235 (2005); J.-M. Lehn, Science **295**, 2400 (2002).

[12] Y. Gu and N. L. Abbott, Phys. Rev. Lett. **85**, 4719 (2000).

[13] D. Pires, J.-B. Fleury, and Y. Galerne, Phys. Rev. Lett. **98**, 247801 (2007).

[14] D. Antypov and D. J. Cleaver, J. Phys.: Condens. Matter **16**, S1887 (2004).

[15] O. Guzman, E. B. Kim, S. Grollau, N. L. Abbott, and J. J. de Pablo, Phys. Rev. Lett. **91**, 235507 (2003).

[16] S. Žumer, *Plenary Talk at the 21st International Liquid Crystal Conference, Keystone, Colorado, July 2–7, 2006*.

[17] T. Araki and H. Tanaka, Phys. Rev. Lett. **97**, 127801 (2006).

[18] M. Ravnik, M. Škarabot, S. Žumer, U. Tkalec, I. Poberaj, D. Babič, N. Osterman, and I. Muševič, Phys. Rev. Lett. **99**, 247801 (2007).

[19] M. Škarabot, M. Ravnik, D. Babič, N. Osterman, I. Poberaj, S. Žumer, I. Muševič, A. Nych, U. Ognysta, and V. Nazarenko, Phys. Rev. E **73**, 021705 (2006).

[20] W. H. Press, B. P. Flannery, S. A. Teukolsky, and W. T. Vetterling, *Numerical Recipes* (Cambridge University Press, Cambridge, 1986).

[21] H. J. Coles, Mol. Cryst. Liq. Cryst. **49**, 67 (1978).

[22] $\Delta t = N\Delta\Gamma\xi^2/L\Gamma \sim 0.2$ ms for $N=3000$ iteration steps, $\Delta\Gamma = 0.4$ relaxation parameter, $\xi = 6.6$ nm nematic correlation length, and $\Gamma = 6.25/\mathrm{Pas}$ rotational viscosity. For the effective viscosity $\eta = 0.1$ Pas was used.

[23] V. G. Veselago, Sov. Phys. Usp. **10**, 509 (1968); J. B. Pendry, Phys. Rev. Lett. **85**, 3966 (2000).